September 1, 1980

An empirical model of quiet dayionospheric electric fields of middle and low latitudes

A. D. Richmond
M. Blanc
B. A. Emery
R. H. Wand
Bela G. Fejer, *Utah State University*, et al.

JOURNAL OF GEOPHYSICAL RESEARCH, VOL. 85, NO. A9, PAGES 4658–4664, SEPTEMBER 1, 1980

An Empirical Model of Quiet-Day Ionospheric Electric Fields at Middle and Low Latitudes

A. D. RICHMOND[1], M. BLANC[2], B. A. EMERY[3], R. H. WAND[4], B. G. FEJER[5], R. F. WOODMAN[6], S. GANGULY[6], P. AMAYENC[2], R. A. BEHNKE[6], C. CALDERON[7], AND J. V. EVANS[4]

Seasonally averaged quiet-day *F* region ionospheric **E** × **B** drift observations from the Millstone Hill, St. Santin, Arecibo, and Jicamarca incoherent scatter radars are used to produce a model of the middle- and low-latitude electric field for solar minimum conditions. A function similar to an electrostatic potential is fitted to the data to provide model values continuous in latitude, longitude, time of day, and day of the year. This model is intended to serve as a reference standard for applications requiring global knowledge of the mean electric field or requiring information at some location removed from the observing radars.

INTRODUCTION

Knowledge of the ionospheric electric field is useful in several branches of upper atmospheric physics. The electric field at middle and low latitudes on magnetically quiet days is believed to be produced mainly by the dynamo action of thermospheric winds [e.g., *Evans,* 1978; *Blanc,* 1979; *Richmond,* 1979], so that knowledge of the electric field can be used to gain further information about the winds and the dynamo mechanism. The electric field causes the ionospheric and plasmaspheric plasmas to drift perpendicular to the geomagnetic field and, consequently, is important for the dynamic variations of these plasmas [e.g., *Matsushita and Tarpley,* 1970; *Roble,* 1975; *Kohl,* 1976; *Richmond,* 1976; *Rishbeth,* 1977; *Murphy et al.,* 1980]. This drifting motion of the ionosphere also affects the dynamics of the thermosphere, both by imparting momentum through collisional interaction [e.g., *Roble et al.,* 1974; *Kohl,* 1976], and by influencing the magnitude of ion drag through redistribution of ionization [e.g., *Anderson and Roble,* 1974]. Knowledge of the global ionospheric electric field is also useful in providing an upper boundary condition on calculations of middle atmosphere electric fields such as those performed by *Roble and Hays* [1979].

Substantial collections of ionospheric electric field data exist for the incoherent scatter radar observatories at Millstone Hill, St. Santin, Arecibo, and Jicamarca. In spite of the large day-to-day variability of the electric fields, earlier analyses were able to determine clear average daily variations [e.g., *Woodman,* 1970, 1972; *Evans,* 1972; *Carpenter and Kirchhoff,* 1974; *Kirchhoff and Carpenter,* 1976; *Richmond,* 1976; *Blanc et al.,* 1977]. More recent analyses have quantified the seasonal and, in the case of Jicamarca, solar cycle variations [*Woodman et al.,* 1977; *Blanc and Amayenc,* 1979; *Fejer et al.,* 1979, 1980; *Wand and Evans,* 1980].

The purpose of this paper is to produce a global model of ionospheric electric fields on quiet days at middle and low latitudes based on incoherent scatter data from the middle 1970's, a period of low solar activity. This model is designed to serve as a reference standard and to provide numerical values of electrodynamic drifts over the entire middle- and low-latitude ionosphere for studies requiring this information.

Richmond [1976] previously produced a global electric field model based on incoherent scatter measurements as well as observations of whistler duct drifts. The number of days of data included in that work, however, was much smaller than that used in the present study. In the present model we are able to include seasonal and, to some extent, longitudinal variations of the electric field, which are not incorporated into *Richmond*'s [1976] model. The present model thus supersedes that earlier one.

DATA BASE

Data are used from the four incoherent scatter radar stations listed in Table 1. These radars measure the ion velocity, whose component **v** perpendicular to the geomagnetic field **B** is related to the electric field **E** by

$$\mathbf{v} = \mathbf{E} \times \mathbf{B}/B^2 \tag{1}$$

At each station, *F* region ionization drifts were typically measured on a few days each month within the interval indicated. Depending on the mode of operation, projections of **v** onto one or more station-dependent axes can be determined at a given time. The measured components of **v** are averaged in height to improve accuracy, a process justified by the expectation that **E** and **v** vary only slightly with altitude within the *F* region, owing to the near-equipotentiality of magnetic field lines and to the large-scale nature of the global electric field. The mean altitude of the measurements is roughly 300 km. All stations except St. Santin determine vector velocities by combining line-of-sight velocities measured at different directions from the transmitter/receiver, corresponding to different volumes of the ionosphere. The assumption is then made that the ionospheric drift vectors are the same for all volumes of measurement from a particular station. For further information about the measurement techniques, see

[1] NOAA Environmental Research Laboratories, Space Environment Laboratory, Boulder, Colorado 80303.
[2] Centre de Recherches en Physique de l'Environnement, Études par Télédetection de l'Environnement, 92131 Issy-les-Moulineaux, France.
[3] National Center for Atmospheric Research, Boulder, Colorado 80307.
[4] Lincoln Laboratory, Massachusetts Institute of Technology, Lexington, Massachusetts 02173.
[5] School of Electrical Engineering, Cornell University, Ithaca, New York 14853.
[6] Arecibo Observatory, Arecibo, Puerto Rico 00612.
[7] Jicamarca Radar Observatory, Instituto Geofisico del Peru, Lima, Peru.

Paper number 80A0414.
0148-0227/80/080A-0414$01.00

TABLE 1. Data Base Information

Station	Geographic Coordinates, deg		Magnetic Coordinates, deg		Period of Observations	Number of Days Used in Averages		
	Latitude	Longitude	Latitude	Longitude		D Months	J Months	E Months
Millstone Hill*	42.6	−71.5	57	1	May 1976 to Nov. 1977	1–11	2–13	0–8
St. Santin	44.1	2.0	40	78	Feb. 1973 to Dec. 1975	5.5–12	1.5–6	3.5–7
Arecibo	18.5	−66.8	31	5	Aug. 1974 to May 1977	2–9	3–14	5–9
Jicamarca	−12.0	−76.9	1	−8	Jan. 1974 to Oct. 1977	2–9†	10–20	5–12
						1–7‡	0–15	0–6

*Geographic coordinates are for radar location; magnetic coordinates are for mean ionospheric location of observations.
†Up.
‡East.

Woodman and Hagfors [1969], *Woodman* [1970, 1972], *Behnke and Harper* [1973], *Harper* [1977], *Blanc et al.* [1977], and *Wand and Evans* [1980].

From each data set, data for magnetically quiet periods are selected according to the criteria of *Blanc and Amayenc* [1979]. In general, periods for which the *Kp* index is 2+ or less are used. However, isolated 3-hour periods with *Kp* values of 3− or 3o are also included if the adjacent 3-hour periods have *Kp* values of 2+ or less; while isolated periods with *Kp* values of 2+ or less are excluded if the adjacent periods have *Kp* values of 3− or greater. (For the east-west drifts at Jicamarca a slightly modified criterion is used in order to have enough data for averaging. In this case, all data for which *Kp* is 3o or less are included, unless there are less than two values available, for which times all available data are included. Because analysis of these data has revealed no noticeable effect of magnetic activity [*Fejer et al.*, 1980], this modification seems warranted.) The selected data are then averaged at each half hour of the day for each of three seasons: *D* months (November–February), *J* months (May–August), and *E* months (March, April, September, October). The number of data included in each average is often a strong function of local time, with more observations at day than at night, and it also depends on the station and on the season. Table 1 lists for each station and season the minimum and maximum number of values used in the averages throughout the day. (At St. Santin the number of values listed in Table 1 corresponds to the number of three-station observations plus one-half the number of two-station observations; see *Blanc et al.* [1977] for a description of the distinction.) Because many more observations of vertical drifts than of east-west drifts were made at Jicamarca, the numbers of observations are listed separately for each component.

Figures 1–4 show the averaged drift components perpendicular to the magnetic field in the upward/poleward and eastward directions for the four stations. The curves in these figures show the fit of our model to the data, as described in the next section. The day-to-day variability of the data used to produce these averages is quite large, generally comparable to the magnitudes of the drifts themselves. The error bars in Figures 1–4 do not indicate this variability but rather indicate the estimated probable error with which the average values can be determined, which for equally weighted data would be the standard deviation divided by the square root of the number of observations entering into a particular average value. Further discussions of seasonally averaged data and of their dispersions for individual stations are given by *Blanc and Amayenc* [1979], *Fejer et al.* [1979, 1980], *Wand and Evans*

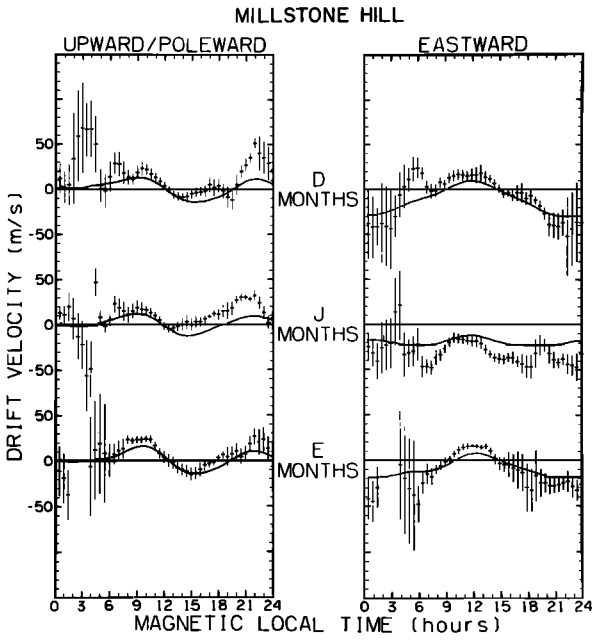

Fig. 1. Seasonally averaged quiet-day drifts (points with error bars) and model drifts (solid lines) perpendicular to the geomagnetic field at 300 km measured at Millstone Hill. Note that the error bars do not represent the magnitude of day-to-day variability (see text).

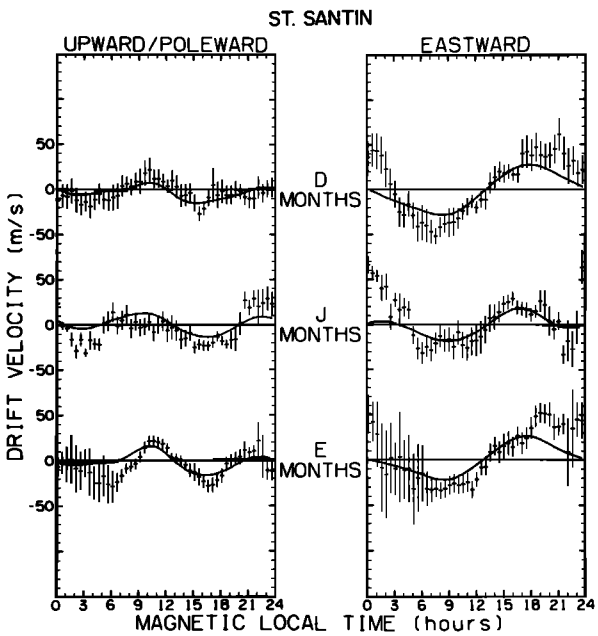

Fig. 2. Same as Figure 1, but for St. Santin.

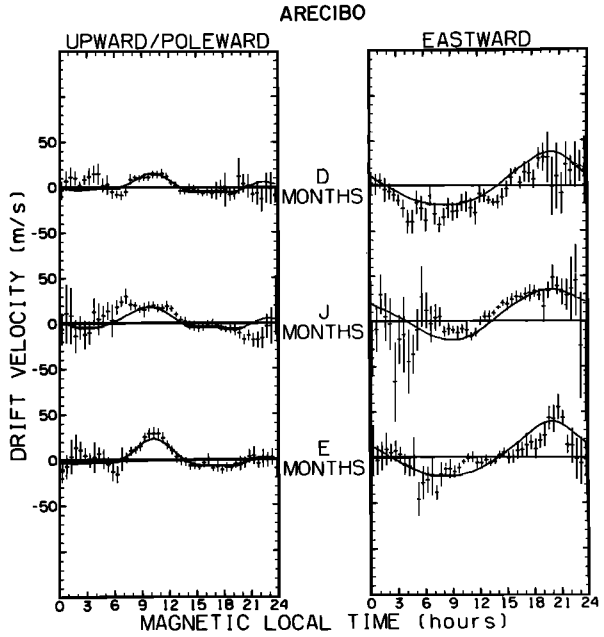

Fig. 3. Same as Figure 1, but for Arecibo.

[1980], S. Ganguly et al. (unpublished manuscript, 1980), and B. A. Emery et al. (unpublished manuscript, 1980).

Empirical Model

We wish to determine a global function which adequately represents the observed drifts at all four stations simultaneously, and also gives a 'reasonable' representation of the drifts to be expected at other locations. It should be obvious that a reasonable representation at locations where no data are available depends to some extent on subjective judgments.

As a first step, we adopt a coordinate system linked to the geomagnetic field. A primary reason for this is that we expect magnetic field lines to be nearly equipotential [e.g., *Dougherty*, 1963; *Peterson et al.*, 1977], so that there is a high degree of correspondence of the transverse electric field between conjugate points in the ionosphere. Magnetic apex coordinates [*Van Zandt et al.*, 1972*a*, *b*] have the desirable properties that conjugate points have the same latitude and longitude coordinates and that all field lines of a given apex latitude peak at the same height above the earth for any longitude (unlike, say, invariant coordinates). Because magnetic apex latitude λ_A is defined to be constant along a magnetic field line and to be zero along the magnetic equator at the earth's surface, at 300-km altitude, λ_A jumps from $-12.24°$ to $+12.24°$ across the magnetic equator. For our fitting procedure it is more convenient to have a magnetic latitude coordinate which goes to zero at the magnetic equator at 300 km, and so we define our magnetic colatitude θ in terms of λ_A as

$$\theta = \sin^{-1}[1.0232475 \cos \lambda_A] \tag{2}$$

whereby our magnetic latitude $(90° - \theta)$ has the same sign as λ_A. Our magnetic longitude ϕ is defined to be identical with magnetic apex longitude ϕ_A, being zero on the geomagnetic prime meridian at the magnetic equator (about 69° west geographic longitude).

We next define a pseudo electrostatic potential Φ' to which our 300-km model drift components $v_\perp$ (perpendicular to the magnetic field in the magnetic poleward/upward direction) and v_ϕ (in the magnetic eastward direction) are related by

$$v_\perp = \frac{-1}{B(\theta)R \sin\theta} \frac{\partial \Phi'}{\partial \phi} \tag{3}$$

$$v_\phi = \frac{-1}{B_0 R \cos\theta} \frac{\partial \Phi'}{\partial \theta} \tag{4}$$

$$B(\theta) = 1/2\ B_0(1 + 3\cos^2\theta)^{1/2} \tag{5}$$

$$B_0 = 5.2 \times 10^{-5}\ T \tag{6}$$

$$R = 6.671 \times 10^6\ m \tag{7}$$

Note that we effectively use a centered dipole magnetic field model to relate the drifts and the pseudopotential. Since the actual geomagnetic field is not dipolar, our pseudopotential is not a true electrostatic potential, nor do our model drifts strictly conserve magnetic flux when interpreted as a magnetic convection model. However, these problems are relatively unimportant in light of other uncertainties in our model. To obtain an estimate of the true electrostatic potential, we would suggest multiplying Φ' by the true local magnetic field strength (averaged with the value at the conjugate point) and dividing by $B(\theta)$ as given by (5). The reason for doing this is based on the theory that the electric field is generated primarily by ionospheric winds blowing across the magnetic field. If the wind strength has no systematic variation with longitude (a simplistic and experimentally unverified assumption), then the electric field strength would tend to vary with longitude as the magnetic field strength, while the drift velocities should tend not to have a systematic longitudinal variation of this nature.

We represent the pseudopotential Φ' as a series of terms:

$$\Phi'(d, T, t, \theta) = \sum_{k=0}^{2} \sum_{l=k-2}^{2-k} \sum_{m=-4}^{4} \sum_{n=|m|}^{7} A_{klmn} P_n^m(\cos\theta) f_m \cdot (\pi t/12\ \text{hours}) f_k(\pi T/12\ \text{hours}) f_{-k}[\pi(d+9)/182.62] \tag{8}$$

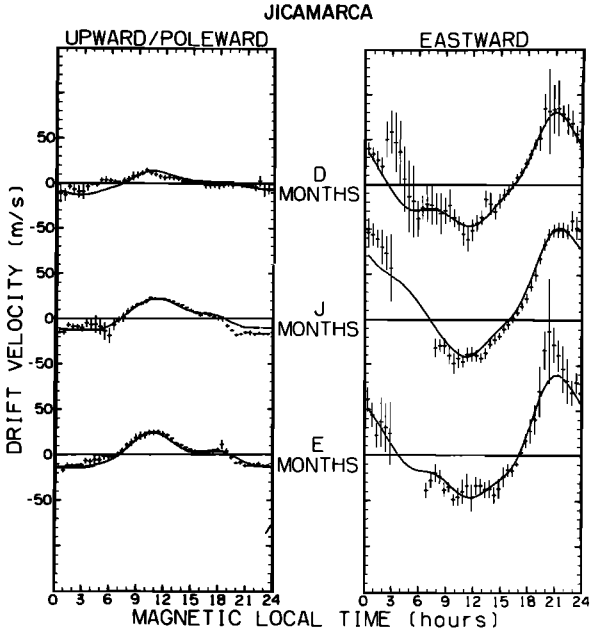

Fig. 4. Same as Figure 1, but for Jicamarca.

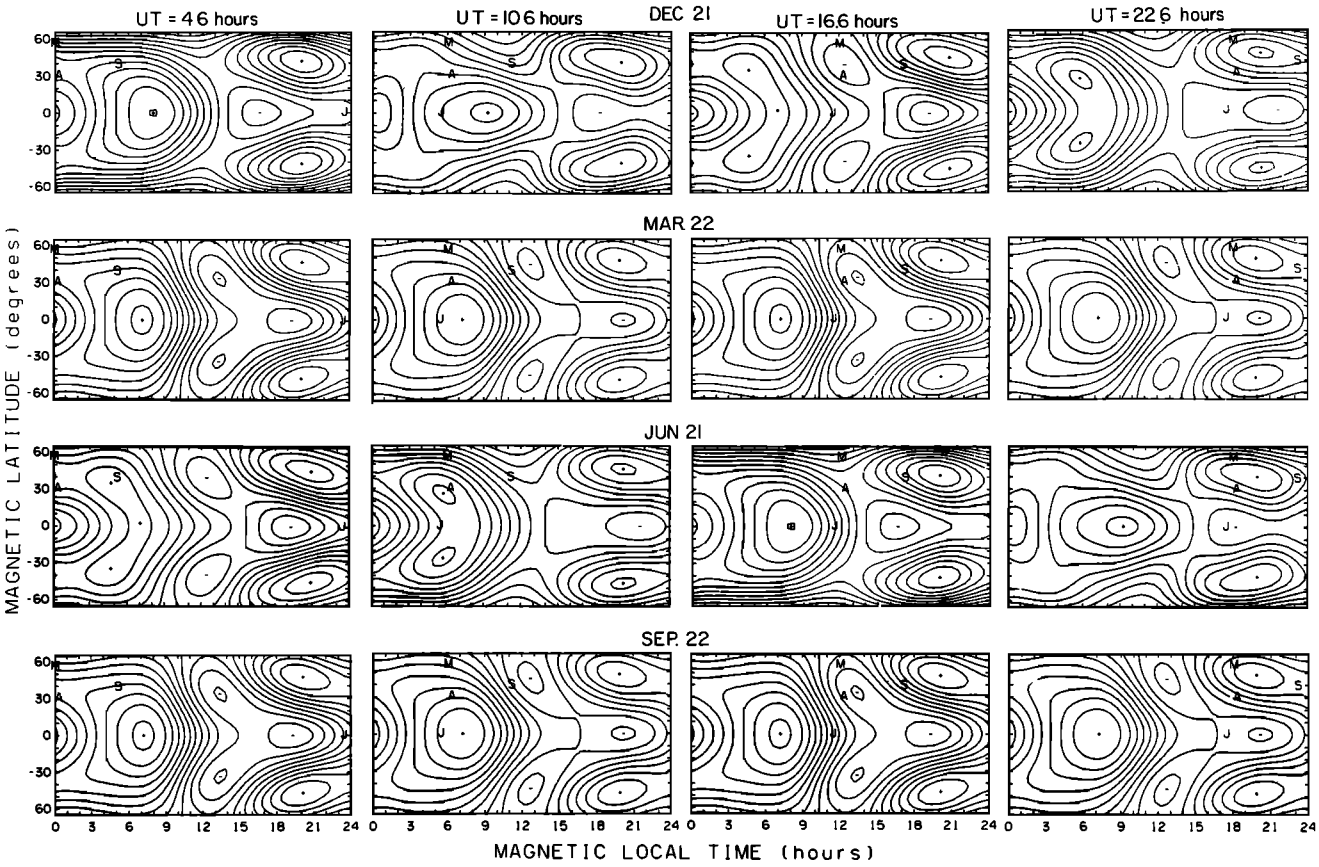

Fig. 5. Magnetic local time–magnetic latitude plots of the 300-km pseudoelectrostatic potential Φ' at four universal times, spaced 6 hours apart, on 4 days of the year, spaced 3 months apart. The contour spacing is 500 V, and maxima and minima are indicated by plus and minus signs. The letters M, S, A, and J show the locations of the four incoherent scatter stations. Values of Φ' above 65° magnetic latitude are not shown, and values at locations far removed from the observing stations are entirely speculative.

$$f_m(\psi) \equiv \sqrt{2} \sin(m\psi) \qquad m > 0$$
$$f_m(\psi) \equiv 1 \qquad m = 0 \qquad (9)$$
$$f_m(\psi) \equiv \sqrt{2} \cos(m\psi) \qquad m < 0$$

where d is day number of the year, T is universal time of the day, and t is magnetic local time (MLT), defined by $T + (\phi - 69°)/(15°/\text{hour})$.

The functions P_n^m and f_m are fully normalized as in the work of *Richmond* [1974]. Within the series (8), a number of the coefficients are automatically set equal to zero. First, all coefficients with $n + m$ odd are eliminated so that Φ' is constrained to be symmetric about the magnetic equator. Second, all coefficients with $k + l$ odd are eliminated. This results in Φ' having characteristics one would expect of an electrostatic potential generated by ionospheric winds with a daily variation independent of geographic longitude, and a seasonal variation symmetric about the geographic equator, blowing in a tilted centered dipole magnetic field. That is, the potential on one side of the earth at the December solstice is identical to that at the opposite side of the earth at the June solstice, and the potential on opposite sides of the earth is identical at the equinoxes. As we have very little information about longitudinal variations of the electric field, this assumption is made for convenience to limit the number of terms in the series. Third, to further limit the terms to a total of 128 (a convenient computer value), coefficients with $n = 7$ are eliminated unless both k and l are zero, and coefficients with $n > 5$ and $|m| = 4$ are eliminated if $|l| = 2$.

We determine values of the coefficients A_{klmn} such that the resultant drift components from (3) and (4) match reasonably well all of the data simultaneously, for each component from each station at each local time for all three seasonal averages. Even with the number of coefficients limited as described above, a wide variety of choices can be made which give satisfactory agreement with the data. However, many of these choices of coefficients give an 'unreasonable' behavior of Φ' at locations far removed from the available stations. We therefore use subjective constraints to limit the magnitude of those terms in (8) with $l \neq 0$, representing universal time (or longitudinal) variations of the local-time pattern. Details of the fitting procedure and a list of the coefficients are given in the appendix.[1]

The curves in Figures 1–4 show the seasonal average values of $v_\perp$ and v_ϕ from our model at the locations of the four stations. The fit to the data is satisfactory, although not excellent. Some of the difficulty in achieving a good fit everywhere arises from the totally different behavior of the east-west drifts observed at Millstone Hill and those observed at St. Santin.

Figure 5 shows maps of the pseudopotential at four differ-

[1] The appendix is available with the entire article on microfiche. Order from the American Geophysical Union, 2000 Florida Avenue, N.W., Washington, D. C. 20009. Document J80-011; $1.00. Payment must accompany order.

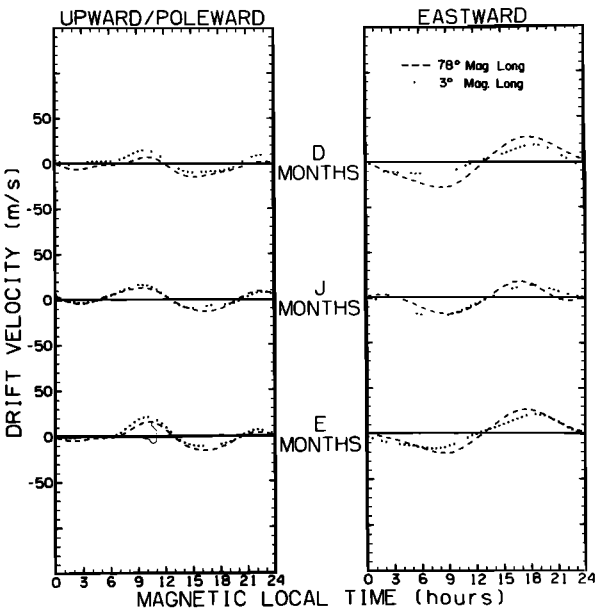

Fig. 6. Seasonally averaged model drifts as a function of magnetic local time at 40° magnetic latitude and at 78° (dashed curves) or 3° (dotted curves) magnetic longitude, at 300-km altitude.

ent universal times for four seasonal epochs. At the time 4.6 UT the antisolar point is approximately on the geomagnetic prime meridian; the other times are spaced at 6-hour intervals from this. The pseudopotential is shown only up to ±65° latitude, because it is incapable of reproducing meaningfully the complex electric fields in the polar regions. (See *Evans et al.* [1980] for some examples of high-latitude electric field maps deduced from incoherent scatter radar data.) The locations of the four stations are indicated by the letters A, J, S, and M. Clearly, the pattern of the pseudopotential in regions distant from these stations is speculative and strongly dependent on assumptions we made in our fitting procedure. However, the variety of patterns in Figure 5 might give some indication of the actual diversity of the quiet-day average ionospheric electric fields.

Our data base should be adequate to permit examination of longitudinal (or UT) variations of the drift patterns at midlatitudes in the North Atlantic region. Figure 6 shows seasonal average drifts at 40° magnetic latitude and at two magnetic longitudes: 78° corresponds to St. Santin, while 3° corresponds to a point between Millstone Hill and Arecibo. The patterns are fairly similar, but a few differences are noticeable. The upward/poleward drift tends to be shifted positive at 3° with respect to that at 78°, at all local times and all seasons. The eastward drift tends to have a larger diurnal amplitude at 78° than at 3°, particularly in the D months.

Our confidence in the reliability of the latitude–local time maps of pseudopotential can be increased by averaging over universal time. The structure of our model is such that the universal-time-averaged pseudopotential varies semiannually. Figure 7 shows maps of the UT-averaged pseudopotential for solstitial and equinoctial conditions, as well as for the average over the year. The yearly average pattern is generally similar to that found by *Richmond* [1976], but there are differences which can be associated with the different data bases used. Figure 8 shows the corresponding UT-averaged drifts at 10° latitude spacings, again for solstitial, equinoctial, and yearly average conditions. A few features of the UT-averaged model drifts are worthy of comment. We confine our attention to the daytime hours, where the data base is more reliable. The daytime amplitude of the upward/poleward drifts is larger at the equinoxes than at the solstices. A significant seasonal variation in the time of maximum drift is also apparent, the solstitial phase being later than the equinoctial at low latitudes, but earlier at higher latitudes. The east-west drifts tend to have a daily mean westward component at higher latitudes and a daily mean eastward component at low latitudes, this tendency being stronger at solstice than at equinox. The daily variation of the east-west drift is primarily diurnal, the amplitude generally decreasing with increasing latitude. The phase of the diurnal variation shifts gradually earlier with increasing latitude up to 40° and then shifts more strongly to earlier times at higher latitudes.

The UT-averaged drifts for equinox are appropriate for comparison with results from the ionospheric dynamo calculations of *Richmond et al.* [1976] and of *Forbes and Lindzen* [1976, 1977], as these studies used equinoctial conductivities in models having no UT variations (owing to the assumed coincidence of geographic and geomagnetic poles). Such a comparison, however, shows substantial disagreements between observed and computed drifts, even though agreement of some features is evident. The disagreement suggests that the wind and/or conductivity models used in the theoretical calculations are inadequate to represent average conditions on a global basis. Such an inadequacy is also suggested by the amount of disagreement between the two theoretical studies. Some insight into how improvements of theoretical dynamo calculations can be made is offered by *Forbes and Garrett* [1979].

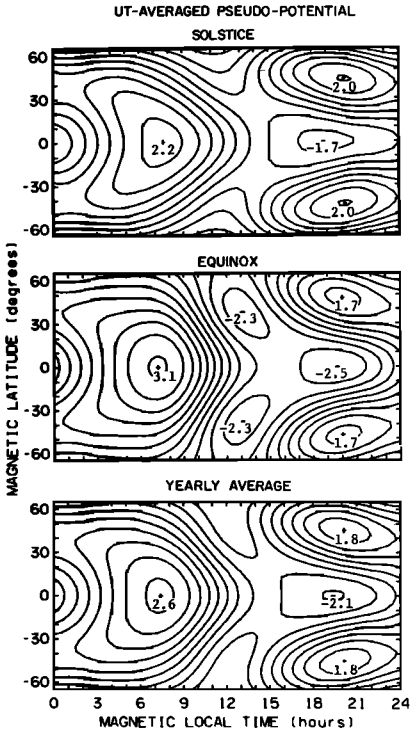

Fig. 7. Magnetic local time–magnetic latitude plots of the UT-averaged pseudopotential at 300 km for (top) solstice conditions ($d = -9$ or 173.62) (middle) equinox conditions ($d = 82.31$ or 262.93), and (bottom) the average over the year. Contour spacing is 500 V. Maxima and minima values are in the kilovolts.

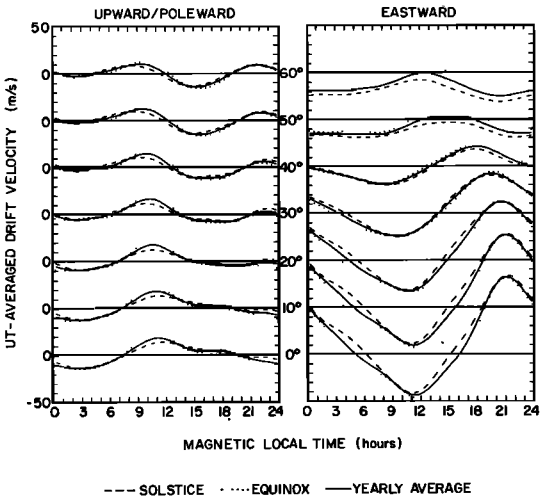

Fig. 8. UT-averaged model drifts as a function of magnetic local time at spacings of 10° magnetic latitude, for solstice conditions (dashed curves), equinox conditions (dotted curves), and the average over the year (solid curves).

DISCUSSION

The model presented here should be useful for applications requiring global information of the average quiet-day ionospheric electric field for solar minimum conditions or for applications requiring a reference electric field at some location far removed from the available observatories. Researchers requiring only information about the electric field near one of the four incoherent scatter radars would do better to use one of the local models of *Blanc and Amayenc* [1979], *Fejer et al.* [1979, 1980], *Wand and Evans* [1980], S. Ganguly et al. (unpublished manuscript, 1980), or B. A. Emery et al. (unpublished manuscript, 1980). For applications requiring model values more detailed than those presented in this report, we have written a general purpose computer subroutine in Fortran which is listed in the appendix and is available on cards upon request.

One final point of clarification may help prevent confusion in making reference to our model. Our basic model is defined by (2)–(7), that is, it is a function of day number and universal time as well as of magnetic local time and magnetic latitude. In this report we have shown certain types of averaging of this model: averaging over seasons in Figures 1–4 and 6, and averaging over universal time (and sometimes over the year) in Figures 7 and 8. When reference is made to seasonal, yearly, and/or UT averages of our model, we suggest that the nature of averaging used be so stated. Thus the solid curves in Figure 8 represent our 'UT average, yearly average model.'

As more ionospheric electric field data are collected, it may be desirable to produce models with greater accuracy and applicability than the present one has. Extensions of the data base to higher latitudes, to other longitude sectors, and to different solar cycle conditions would clearly be of value.

Acknowledgments. A. D. R. is a Research Associate of the Cooperative Institute for Research in Environmental Sciences, University of Colorado. The Arecibo data used in this study were supplied to the World Data Center A by R. M. Harper.

REFERENCES

Anderson, D. N., and R. G. Roble, The effect of vertical $E \times B$ ionospheric drifts on F region neutral winds in the low-latitude thermosphere, *J. Geophys. Res., 79,* 5231–5236, 1974.

Behnke, R. A., and R. M. Harper, Vector measurements of F region ion transport at Arecibo, *J. Geophys. Res., 78,* 8222–8234, 1973.

Blanc, M., Electrodynamics of the ionosphere from incoherent scatter: A review, *J. Geomagn. Geoelec., 31,* 137–164, 1979.

Blanc, M., and P. Amayenc, Seasonal variations of the ionospheric $E \times B$ drifts above Saint-Santin on quiet days, *J. Geophys. Res., 84,* 2691–2704, 1979.

Blanc, M., P. Amayenc, P. Bauer, and C. Taieb, Electric field induced drifts from the French incoherent scatter facility, *J. Geophys. Res., 82,* 87–97, 1977.

Carpenter, L. A., and V. W. J. H. Kirchhoff, Daytime three-dimensional drifts at Millstone Hill Observatory, *Radio Sci., 9,* 217–222, 1974.

Dougherty, J. P., Some comments on dynamo theory, *J. Geophys. Res., 68,* 2383–2384, 1963.

Evans, J. V., Measurements of horizontal drifts in the E and F regions at Millstone Hill, *J. Geophys. Res., 77,* 2341–2352, 1972.

Evans, J. V., Incoherent scatter contributions to studies of the dynamics of the lower thermosphere, *Rev. Geophys. Space Phys., 16,* 195–216, 1978.

Evans, J. V., J. M. Holt, W. L. Oliver, and R. H. Wand, Millstone Hill incoherent scatter observations of auroral convection over $60° \leq \Lambda \leq 75°$, 2, Initial results, *J. Geophys. Res., 85,* 41–54, 1980.

Fejer, B. G., D. T. Farley, R. F. Woodman, and C. Calderon, Dependence of equatorial F region vertical drifts on season and solar cycle, *J. Geophys. Res., 84,* 5792–5796, 1979.

Fejer, B. G., D. T. Farley, C. A. Gonzales, R. F. Woodman, and C. Calderon, F region east-west drifts at Jicamarca, submitted to *J. Geophys. Res.,* 1980.

Forbes, J. M., and H. B. Garrett, Solar tidal wind structures and the E-region dynamo, *J. Geomagn. Geoelec., 31,* 173–182, 1979.

Forbes, J. M., and R. S. Lindzen, Atmospheric solar tides and their electrodynamic effects, 1, The global Sq current system, *J. Atmos. Terr. Phys., 38,* 897–910, 1976.

Forbes, J. M., and R. S. Lindzen, Atmospheric solar tides and their electrodynamic effects, III, The polarization electric field, *J. Atmos. Terr. Phys., 39,* 1369–1377, 1977.

Harper, R. M., Tidal winds in the 100- to 200-km region at Arecibo, *J. Geophys. Res., 82,* 3243–3250, 1977.

Kirchhoff, V. W. J. H., and L. A. Carpenter, The day-to-day variability in ionospheric electric fields and currents, *J. Geophys. Res., 81,* 2737–2742, 1976.

Kohl, H., F-region dynamics, *J. Atmos. Terr. Phys., 33,* 879–885, 1976.

Matsushita, S., and J. D. Tarpley, Effects of dynamo-region electric fields on the magnetosphere, *J. Geophys. Res., 75,* 5433–5443, 1970.

Murphy, J. A., G. J. Bailey, and R. J. Moffett, A theoretical study of the effects of quiet time electromagnetic drifts on the behavior of thermal plasma at mid-latitudes, *J. Geophys. Res., 85,* 1979–1986, 1980.

Peterson, W. K., J. P. Doering, T. A. Potemra, C. O. Bostrom, L. H. Brace, R. A. Heelis, and W. B. Hanson, Measurement of magnetic field aligned potential differences using high resolution conjugate photoelectron energy spectra, *Geophys. Res. Lett., 4,* 373–376, 1977.

Richmond, A. D., The computation of magnetic effects of field-aligned magnetospheric currents, *J. Atmos. Terr. Phys., 36,* 245–252, 1974.

Richmond, A. D., Electric field in the ionosphere and plasmasphere on quiet days, *J. Geophys. Res., 81,* 1447–1450, 1976.

Richmond, A. D., Ionospheric wind dynamo theory: A review, *J. Geomagn. Geoelec., 31,* 287–310, 1979.

Richmond, A. D., S. Matsushita, and J. D. Tarpley, On the production mechanism of electric currents and fields in the ionosphere, *J. Geophys. Res., 81,* 547–555, 1976.

Rishbeth, H., Dynamics of the equatorial F-region, *J. Atmos. Terr. Phys., 39,* 1159–1168, 1977.

Roble, R. G., The calculated and observed diurnal variation of the ionosphere over Millstone Hill on 23–24 March 1970, *Planet. Space Sci., 23,* 1017–1033, 1975.

Roble, R. G., and P. B. Hays, A quasi-static model of global atmospheric electricity, 2, Electrical coupling between the upper and lower atmosphere, *J. Geophys. Res., 84,* 7247–7256, 1979.

Roble, R. G., B. A. Emery, J. E. Salah, and P. B. Hays, Diurnal variation of the neutral thermospheric winds determined from incoherent scatter radar data, *J. Geophys. Res., 79,* 2868–2876, 1974.

Van Zandt, T. E., W. L. Clark, and J. M. Warnock, Magnetic apex coordinates: A magnetic coordinate system for the ionospheric $F2$

layer, *Tech. Rep. ERL 222-AL 6,* NOAA, U.S. Dep. of Commerce, Boulder, Colo. 1972*a*.

Van Zandt, T. E., W. L. Clark, and J. M. Warnock, Magnetic apex coordinates: A magnetic coordinate system for the ionospheric F_2 layer, *J. Geophys. Res., 77,* 2406–2411, 1972*b*.

Wand, R. H., and J. V. Evans, Seasonal and magnetic activity variations of *F* region electric fields over Millstone Hill, submitted to *J. Geophys. Res.,* 1980.

Woodman, R. F., Vertical drift velocities and east-west electric fields at the magnetic equator, *J. Geophys. Res., 75,* 6249–6259, 1970.

Woodman, R. F., East-west ionospheric drifts at the magnetic equator, *Space Res., 12,* 969–974, 1972.

Woodman, R. F., and T. Hagfors, Methods for the measurement of vertical ionospheric motions near the magnetic equator by incoherent scattering, *J. Geophys. Res., 74,* 1205–1212, 1969.

Woodman, R. F., R. G. Rastogi, and C. Calderon, Solar cycle effects on the electric fields in the equatorial ionosphere, *J. Geophys. Res., 82,* 5257–5261, 1977.

(Received February 19, 1980;
revised March 21, 1980;
accepted March 21, 1980.)